

1 Consistency in body size frequency among hundreds of marine 2 fishes with diverse life histories

3 *Freddie J. Heather¹, Shane A. Richards², Nils C. Krueck¹, Rick D. Stuart-Smith¹, Simon J. Brandl³, Jordan M.
4 Casey³, Graham J. Edgar¹, Neville Barrett¹, Valeriano Parravicini^{4,5}, Asta Audzijonyte^{1,6}*

5 1. Institute for Marine and Antarctic Studies, University of Tasmania, Hobart, Australia

6 2. School of Natural Sciences, University of Tasmania, Hobart, Australia

7 3. Department of Marine Science, The University of Texas at Austin, Marine Science Institute, Port Aransas, TX
8 78373, USA

9 4. PSL Université Paris: EPHE-UPVD-CNRS, Université de Perpignan, Perpignan, France

10 5. Laboratoire d'Excellence "CORAIL", Perpignan, France

11 6. Centre for Marine Socioecology, Tasmania, Australia

12 Abstract

13 Animal body size distributions are shaped by complex interactions among growth, mortality and recruitment.
14 Theoretical expectations of fish body size distributions, derived from growth (k) and mortality (M) rates, are
15 extensively used in fish stock assessments worldwide, yet rely on two life-history parameters (M and k) that
16 are difficult to estimate. Using survey data for 822 species (3,228 populations) of shallow water marine fishes,
17 we show that observed body length distributions can be reconstructed in the absence of these two
18 parameters, and instead using only a single body length metric of a population (e.g., the mean or asymptotic
19 body length). When scaled to the mean of the population, the frequency of body lengths from temporally
20 pooled samples showed a consistent unimodal shape, which could be approximated by the truncated normal
21 or lognormal distribution with a coefficient of variation value of around 0.3. This observation was evident for
22 species with diverse life histories spanning two orders of magnitude in maximum body length. The consistency
23 in population and species-level body length distributions suggests evolutionary convergence on a narrow
24 range of viable outcomes even though multiple intrinsic and extrinsic factors are expected to influence body
25 sizes. The reconstruction of fish body length distributions without knowledge of growth and mortality rates
26 has important implications for the assessment and management of data-poor coastal fisheries worldwide.

27 Significance

28 Scientists have long debated whether size distributions of fish (and other animals with indeterminate growth)
29 follow general rules or are highly variable. Using continental scale observations from hundreds of coastal
30 fishes, we demonstrate remarkable consistency in the shape of length frequency distributions across
31 populations and species with vastly different body sizes and life-histories. This similarity of species and
32 population level body size distributions supports life-history predictions that variation in growth and mortality
33 is constrained to optimize.

34

35

36 Main

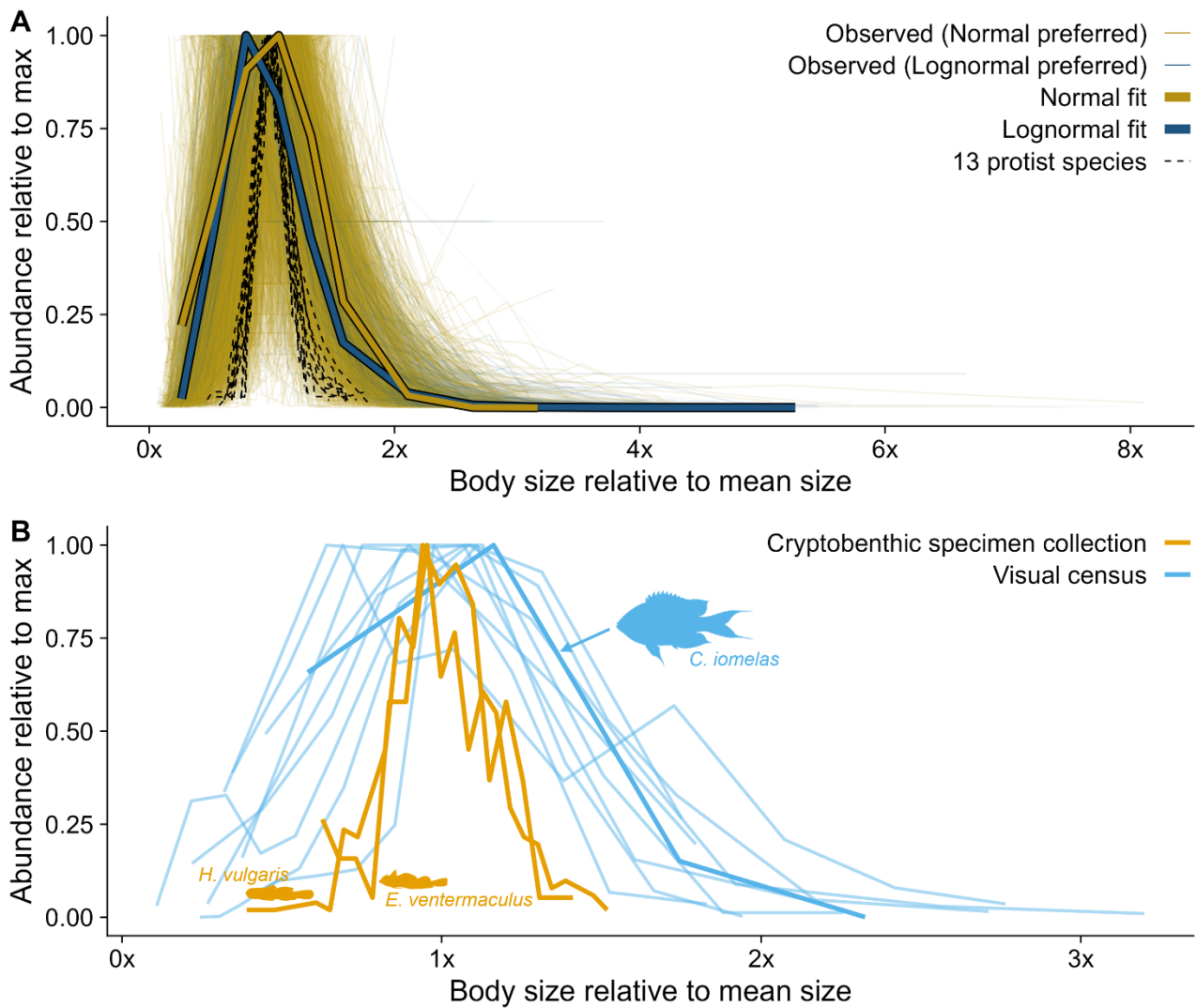
37 The distribution of individual body sizes within animal populations depends on interacting rates of
38 reproduction, recruitment, growth, mortality, and energy allocation^{1,2}. Although the large number of
39 physiological, demographic, and ecological processes influencing body size could potentially lead to high
40 variation in the shape of body size distributions among populations and species, the viable set of growth and
41 mortality characteristics in natural populations is limited^{3,4}. For example, slow growth combined with high
42 mortality may lead to extinction, whereas fast growth and low mortality may be impossible, given that fast
43 resource acquisition demands elevated metabolism and increased predation risk⁵⁻⁷. Many life-history
44 parameters, such as maturation or maximum size, growth, natural mortality and maximum age, show similar
45 and predictable relationships across a wide range of animal taxa^{6,8-12}. Thus, body size distributions, which
46 emerge from these processes, may also show consistent shapes in natural populations. A strong consistency in
47 body size distributions has been suggested for 13 species of unicellular organisms grown in experimental
48 conditions. Despite an order of magnitude difference in the overall species-level mean cell diameter, scaled
49 distributions of protists were remarkably similar and could be described by a single parameter, mean
50 population body size¹³. Similar general patterns in intra-specific body size distributions might emerge across a
51 range of other organisms. For example, in the case of fishes, predictions about body size distributions have
52 been formalized from life-history theory rules, suggesting that for a given set of reproduction, mortality and
53 growth parameters, emergent intra-specific size frequencies will look similar^{2,14-16}. However, reproduction,
54 mortality and growth parameters are unknown for most species and it remains debated whether general
55 patterns in these parameters, and consequently in the shapes of body size frequency distributions, can be
56 expected¹⁷.

57 Understanding and predicting natural body size distributions of fishes is important from both theoretical and
58 applied perspectives. Fishes are the most diverse group of vertebrates, encompassing species of different sizes
59 and life-histories. Critically, they also represent the largest source of non-farmed animal protein, essential
60 nutrition, and income for humans worldwide¹⁸. Fisheries are generally size-selective, often targeting the
61 largest-bodied individuals within a species or population first. The relative abundance of individuals across the
62 size spectrum of a species can be analyzed to infer fishery-induced population depletion, representing a
63 commonly applied basis for stock assessments worldwide. Yet, estimating depletion requires knowledge about
64 expected unfished size frequencies, which remain unknown for the vast majority of fish species. To assess
65 whether population and species level size distributions of natural fish populations show predictable patterns,
66 we used data collected from shallow water reef ecosystems through two divergent methods: underwater
67 visual census observations and exhaustive sampling of, generally smaller-bodied, cryptobenthic fishes. The two
68 data sources comprise 3,228 populations of 822, mostly unfished, temperate and tropical reef fish species that
69 span a broad range of ecological and life-history traits¹⁹ as well as maximum body lengths ranging from 1.1 cm
70 to 2.5 meters.

71 Results and discussion

72 Despite the multitude of processes expected to influence individuals of different body sizes within a
73 population, the observed length distributions of all 3,228 populations were remarkably similar in shape (after
74 scaling individual body lengths by the population mean length to allow direct comparison among species of
75 varying sizes; Fig. 1). Across three spatial scales and assumed organizational levels (population-level,
76 metapopulation-level, and whole species-level; see Methods), and both sampling methods, most observed
77 length distributions (98%) were approximately unimodal or hump-shaped.

78 For these 98% of populations ($n = 3,166$) we fit two common statistical distributions, the normal (truncated at
79 the lowest observable size classes) and lognormal (median distribution fits in Fig. 1A), to the length-frequency
80 data. Bayesian methods were used to assess which of the two distributions better described the observations,
81 and to estimate their mean and coefficient of variation (CV). Most populations (93% of the cryptobenthic
82 fishes, $n = 127$ populations, and 89% of larger bodies species in visual census surveys, $n = 2,571$ populations)
83 were better described by a truncated normal distribution (Extended Data Fig. 1). Yet, regardless of the best
84 fitting distribution, the relative spread (i.e., CV) around the mean body length was similar across populations
85 and species (Fig. 2). For larger fish, analyzed through visual census, 80% of CV estimates were between 0.22
86 and 0.52 for the truncated normal distribution and between 0.27 and 0.51 for the lognormal distribution (95%
87 of estimates from 0.19 to 0.55 and 0.24 to 0.58, respectively) (Fig. 2). The median CV values for the normal and
88 lognormal distributions were very similar at 0.34 (SE = 0.002) and 0.37 (SE = 0.006), respectively. For the
89 smaller, cryptobenthic fish populations and species, variation in body size was slightly lower (e.g. see Figs. 1B
90 and 2), with the median value of the normal distribution CV at 0.23 (only 9 populations were better described
91 by the lognormal distribution). The difference in CVs between small cryptobenthic and larger visual census
92 species was partially explained by different observation methods and the binning of visual census data (versus
93 individual measurements to the nearest mm for the cryptobenthic species). When cryptobenthic fish data
94 were placed into bins similar to the visual census data, their CVs increased from the median CV value of 0.23 to
95 0.28 (Extended Data Fig. 2).

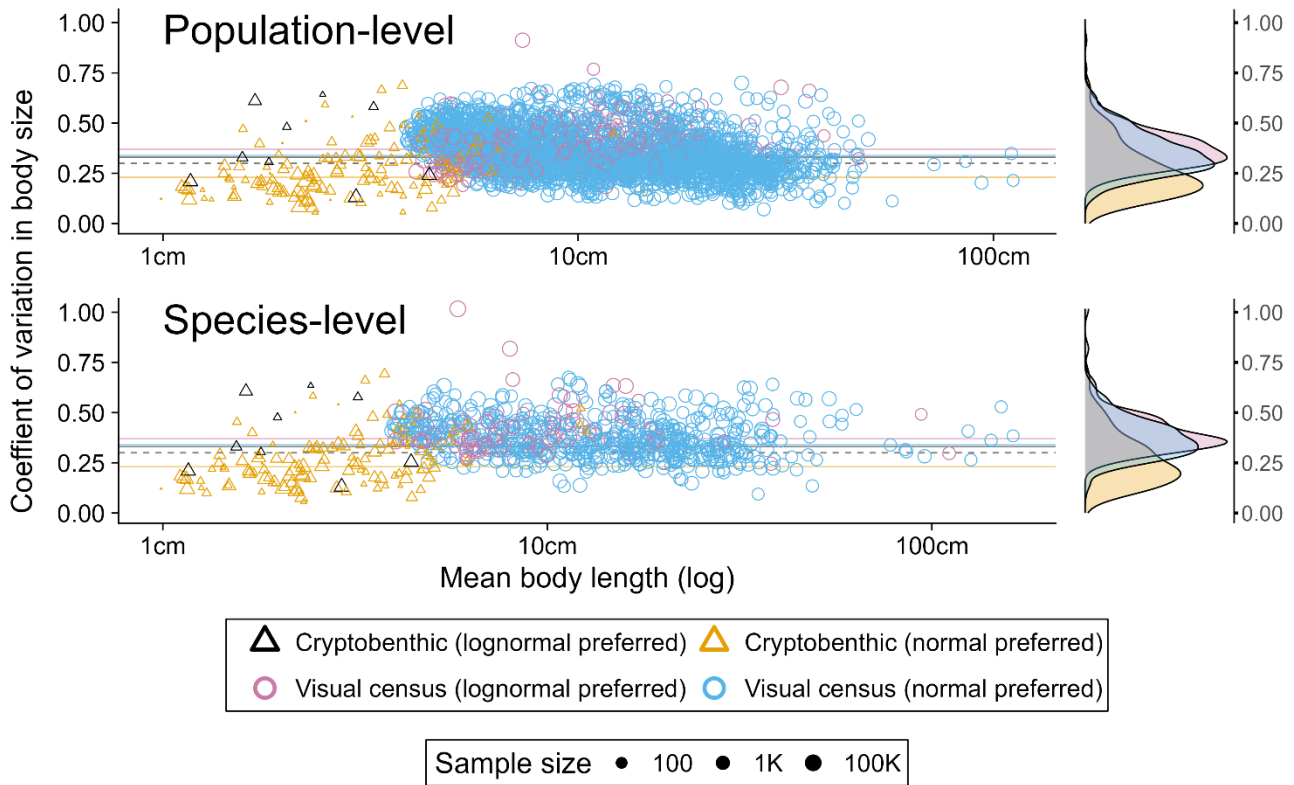


96

97 **Figure 1: Observed body length distributions across 3,228 fish populations show a similar unimodal shape.** A)
 98 Observed individual body length distributions shown in thin solid lines with the median parameter estimates
 99 from normal-preferred and lognormal-preferred model fits shown as thick yellow and dark blue lines,
 100 respectively. Dashed lines in (A) show scaled body size (cell diameter) distributions of 13 freshwater protist
 101 species extracted from Giometto et al. (2013). B) A random selection of 12 populations for visualisation
 102 purposes; three species have been highlighted (thicker lines) to indicate that each line represents a population-
 103 level body length distribution. Binned body length data were normalized to the bin width to allow comparison
 104 with continuous body length data. Abundance density (y-axis) is scaled to the maximum abundance density of
 105 the population, and body size (x-axis) is scaled to the mean body size of the population.

106 The estimated CV values for fish length were consistent across three different spatial scales: population-level
 107 (Fig. 2), metapopulation or ecoregion-level²⁰ (Extended Data Fig. 3), and the entire species-level (Fig. 2). The
 108 results were also similar when species that may be targeted by recreational or commercial fisheries (12% of
 109 total, n = 97 species) were removed from the analysis (Extended Data Fig. 4). Naturally, over short temporal
 110 and fine spatial scales, local recruitment and mortality events might increase the variability of size distributions
 111 and produce multimodal size frequencies, such as sometimes seen in fisheries samples, especially from highly
 112 seasonal species^{21,22}. Multi-modality is likely to be rarer when body size data encompasses multiple sampling

113 events and when seasonality is weaker, as is the case for our data. Only about 2% of coral reef and temperate
 114 rocky reef populations in our dataset revealed multiple peaks in body length frequencies (Extended Data Figs.
 115 5).
 116



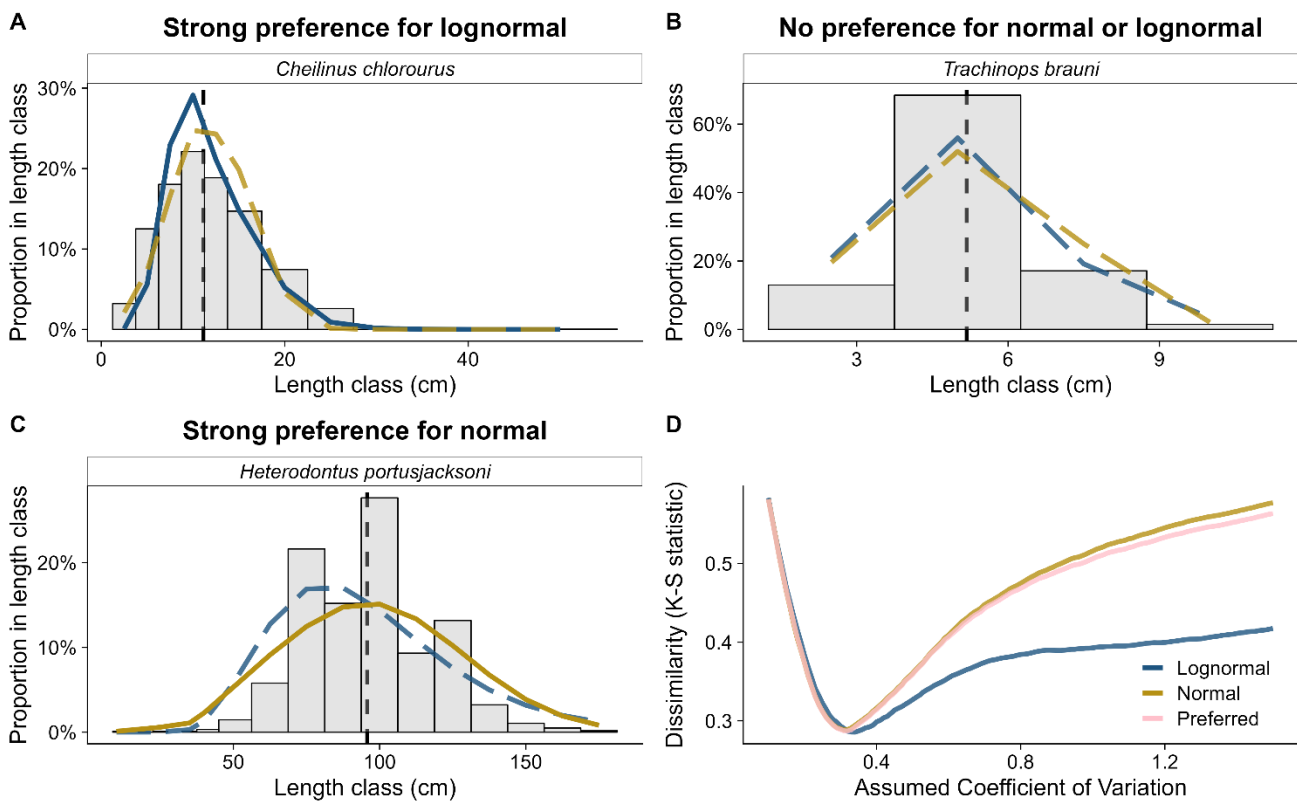
117

118 **Figure 2: Coefficient of variation (CV) of body length distributions of ca 3000 fish populations of larger**
 119 **bodied species (visual census and largest cryptobenthic fish) is approximately 0.34, regardless of the mean**
 120 **body length of the population and the assumed statistical distribution.** Each symbol shows the CV value of a
 121 single fish population (grid cell, see Methods) or species. The color and shape of the symbol indicates the
 122 better-fitting statistical distribution and the sampling method. CV (y-axis) is calculated as the median of the
 123 posterior parameters associated with the better-fit distribution. Colored horizontal lines represent the median
 124 CV values, dashed line shows the estimated CV value of protists from Giometto et al.¹³. Marginal density plots
 125 show the distribution of CV values across populations; for cryptobenthic lognormal preferred (black triangles),
 126 marginal plots are not shown due to small sample sizes ($n = 9$ populations). Symbol size is relative to the
 127 sample size (log scale).

128 Across nearly two orders of magnitude in mean body length, the relative variation around the mean in the size
 129 distribution of fish species was largely independent of the mean body size (Fig. 2). The smallest cryptobenthic
 130 species revealed slightly lower variability in body sizes, while populations of the larger cryptobenthic species
 131 (mean body length > 5 cm) were mostly consistent with the level of variability observed in the visual census
 132 dataset (even before accounting for the binning). Tiny cryptobenthic species, such as *Eviota* spp.²³ (Extended
 133 Data Fig. 6), represent an extreme range of fish life-histories, with high mortality rates, rapid growth
 134 throughout their lives, and unique demographic dynamics²⁴. Physiological and ecological constraints may
 135 eliminate larger individuals of cryptobenthic species and reduce body length variation within this group.

136 Interestingly, body size variability in 13 experimentally grown protists species¹³ was also similar to those of the
 137 fish studied here, with the CV of cell diameter at ca 0.3 (dashed lines in Figs. 1A and 2). These findings suggest
 138 that body size distributions of many other organisms might be well-approximated with normal or lognormal
 139 distributions and a relatively narrow range of associated CV values. This universality has important theoretical
 140 and ecological implications and should be further investigated with a broader dataset of natural population
 141 body size data across taxa, sampling methods, and habitats.

142 Assuming a CV value other than 0.34 produced a worse fitting distribution. We tested this claim using
 143 calculations of dissimilarity (Kolmogorov-Smirnov test) by comparing the predictions of the simple single-
 144 parameter model using a range of CV values with the observed body length distributions. Assuming other CV
 145 values quickly reduced the predictive power (Fig. 3D). Importantly, when a CV of 0.34 was used, predictive
 146 power was similar regardless of which underlying statistical distribution (truncated normal or lognormal) was
 147 used to approximate the observed size distribution (Fig. 3). This is a useful property because the best suited
 148 statistical distribution would generally be unknown.



149

150 **Figure 3: Empirical body size distributions (grey bars) can be reconstructed from the mean body size of the**
 151 **population (vertical black dashed line) and assumed CV of 0.34.** Panels A-C show randomly selected
 152 populations from one of three population groups for which body size distributions were best described by
 153 lognormal, normal or either of the two statistical distributions. Grey bars show observed data and lines show
 154 predicted distributions assuming either truncated normal or lognormal statistical distribution and CV of 0.34.
 155 Panel D shows that assuming CV of 0.34 provides the best fitting distributions with lowest median Kolmogorov-
 156 Smirnov (K-S) statistic across all populations regardless of the assumed statistical distribution (lognormal for all
 157 3000 populations, truncated normal for all, or estimated using the best fitting distribution). Lower or higher CV
 158 values quickly reduced the predictive power, shown by higher K-S values.

159 Fish population dynamics theory and expectations about body size distributions under different growth and
160 mortality rates were originally formulated by Beverton and Holt¹⁴ in the mid-20th century and later
161 operationalized in size-based stock status assessment models by Hordyk *et al.*^{2,15} and Froese *et al.*¹⁶. According
162 to classic theory, the shape of a scaled body size distribution is flexible and determined by the relationship
163 between mortality (M) and growth (k)^{15,16}. Empirically estimated M/k ratios across species and phylogenetic
164 groups vary between at least 0.5 and 3.0^{2,12,17,25}, although estimates of both M and k are notoriously hard to
165 obtain. In fact, both life-history parameters are available for only around 17% of 7000 exploited species of
166 fishes globally²⁶, and even for these species parameter values remain uncertain¹⁷. This long-standing challenge
167 undermines the robustness of stock assessments, including applications of size-based approaches for data-
168 poor conditions, hindering the effective management of world fisheries.

169 The similarity of shapes in body size distributions observed here (i.e., a narrow range of CV values) suggests
170 that M/k ratios in natural populations might be constrained. In fact, such constraints have been proposed
171 earlier, including estimates of an evolutionary optimal M/k ratio of 1.5, which is often used as a default
172 assumption for stock assessment applications investigating poorly researched fish species^{11,26,27}. However,
173 whether an M/k ratio of 1.5 is optimal or broadly representative is under debate^{28,29}, and empirical tests are
174 limited because traditional fish body size datasets have been confined to economically important fishery
175 species, for which unfished body size distributions are generally unknown. With more widespread application
176 of underwater videos and diver-based survey methods, the availability of datasets from all fish species in a
177 community opens new possibilities to test and expand fish population dynamics theory. Overall, our findings
178 suggest that across a broad range of environmental conditions, from tropical to temperate reefs,
179 environmental and demographic parameters shaping growth and mortality are likely constrained, resulting in
180 similar relative abundances of small, medium, and large individuals in unharvested populations. Yet the direct
181 comparison between consistent CV values reported here and estimated M/k ratios in previous work is not
182 straightforward. For example, even species with very low estimated M/k ratios (e.g. long-lived and relatively
183 early maturing sea sweep, *Scorpiis aequipinus*, or banded morwong, *Chirodactylus spectabilis*^{25,30}) had CV
184 values close to the median value in our dataset (Extended Data Fig. 6).

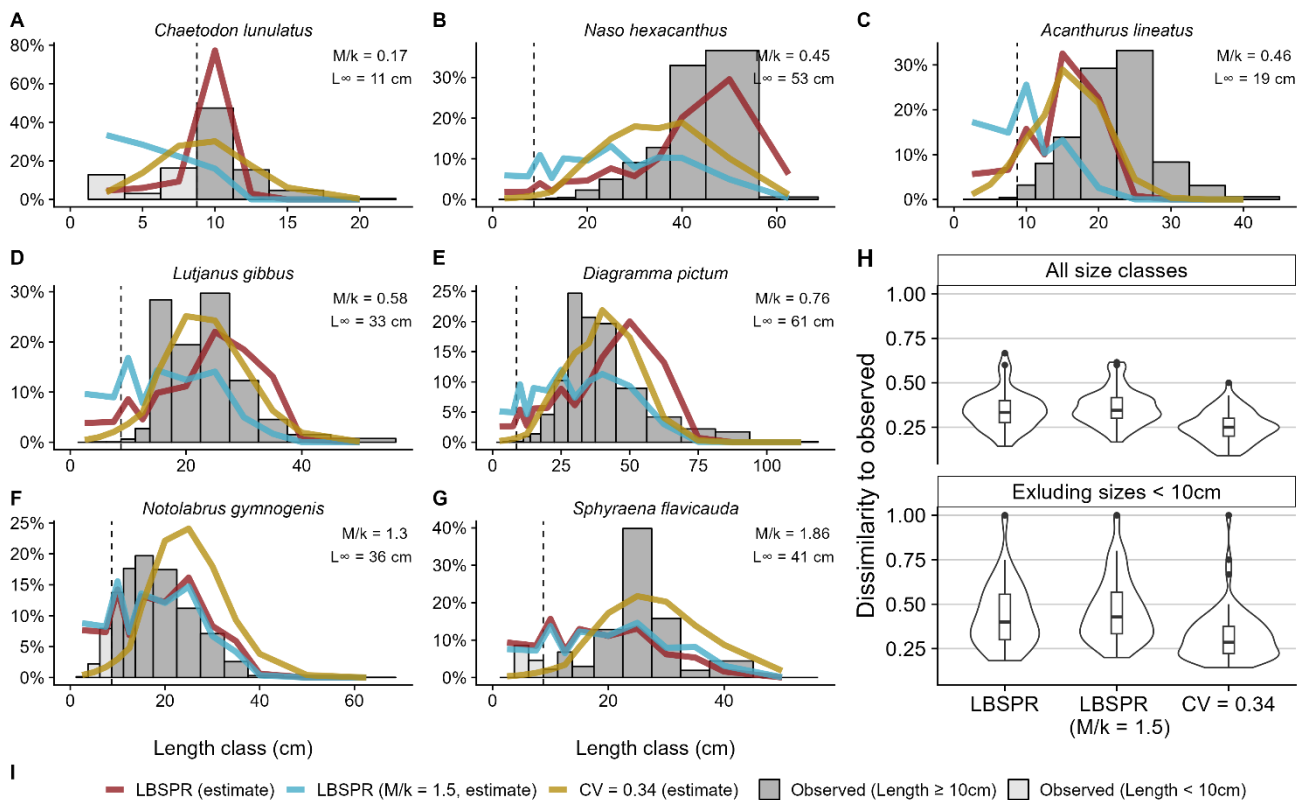
185 More importantly, the relatively consistent CV values observed in our study across multiple populations and
186 species, and across a range of body sizes, suggests that even without prior information on life-history
187 parameters, a single parameter – mean body length (or its approximation from the asymptotic length, see
188 Methods and Extended Data Fig. 7) – allows for a sufficiently accurate assessment of observed (i.e., post-
189 recruitment) body length distributions for many fish populations and species. To assess the performance of
190 our simple method against a more complex population model we compared visual survey observations (grey
191 bars in Fig. 4) to expected distributions generated using fish population dynamics theory^{2,14,15}, as implemented
192 in a widely used length-based population assessment model¹⁵ (the length-based spawning potential ratio,
193 LBSPR, estimation approach, red line in Fig. 4). The theoretical prediction of length-frequency distributions
194 based on LBSPR requires knowledge of three critical life-history parameters - asymptotic body length (L_{inf}) and
195 the ratio between mortality rate (M) and the von Bertalanffy growth coefficient (k). The method further
196 assumes continuous recruitment and constant length variability around mean size at age (default CV value is
197 0.1). The alternative approach derived from findings in this study requires only a single parameter - asymptotic
198 body length L_{inf} (same as for the LBSPR based predictions) - which is then used to estimate mean body length
199 (Extended Data Fig. 7) and assumes a truncated normal size distributions with a CV of body length of 0.34.

200 The life-history parameters required for LBSPR analyses were available for 68 (out of our 822) species that are
201 unlikely to be intensively fished, all from the visual census data. We found that for these 68 species the LBSPR
202 model approximated the observed body size distributions reasonably well (grey bars and red line in Fig. 4 A-G),

203 largely returning unimodal, hump shaped body size distributions as observed. However, length distributions
 204 reconstructed from just the asymptotic body length and an assumed CV value of 0.34 (made on a continuous
 205 scale, then clustered into bins corresponding to empirical data) provided a similarly good, or even better, fit.
 206 The dissimilarity between predictions and observations (based on Kolmogorov-Smirnov test) was generally
 207 lower for the simple method (in all cases assumed asymptotic length was the same between the two
 208 methods). This was true regardless of whether comparisons were done on all fish size classes or whether
 209 individuals <10cm were excluded due to possible observation bias in the data (Fig. 4H). Using a generic M/k
 210 ratio of 1.5 (see Froese et al.¹⁶), rather than species-specific growth and mortality parameters¹⁷, did not
 211 noticeably change the LBSPR model predictions (Fig. 4H).

212 As expected, the LBSPR model predicted slightly higher abundances for the smallest size classes (<10cm) than
 213 observed, which could either indicate incorrect modelling assumptions or, more likely, sampling selectivity in
 214 our data (Extended Data Fig. 8). Visual census is inevitably subject to observation bias because divers are
 215 unlikely to reliably detect the smallest individuals³¹. Sampling bias is likely to be considerably smaller in the
 216 exhaustively sampled cryptobenthic fishes, although this assumption could not be assessed here, since life-
 217 history parameters required for theoretical predictions remain unknown for most cryptobenthic species. Yet,
 218 regardless of the sampling method, the smallest body size range, represented by eggs and larvae, often occur
 219 in locations that are difficult to study (i.e., the open ocean), and thus cannot be accurately observed. As such,
 220 generalizations about body length distributions presented here refer to the observable, post-recruitment life
 221 stages of reef fish populations, which are also of the highest relevance for reef ecosystems and associated
 222 fisheries.

223



224

225 **Figure 4: Simple one parameter model that assumes truncated normal distribution and $CV = 0.34$ matches**
226 **observations similarly well or better than commonly used size-based methods with more parameters**
227 **(LBSPR). Panels A-G shows observations (grey bars) and predictions (solid lines) for seven randomly selected**
228 **(from 68 species with available life-history parameters). Predictions are shown for a simple method using**
229 **truncated normal distribution (yellow) with a $CV = 0.34$ and from LBSPR using either empirically estimate M**
230 **and k values from Prince et al.¹⁷ (red) or assuming a generic M/k ratio of 1.5^{16} . Panel H shows the dissimilarity**
231 **(Kolmogorov-Smirnov statistic) between the prediction and the observed body size distribution for all 68 species**
232 **using all size classes or removing individuals that may have observational sampling bias (less than 10cm in**
233 **body length).**

234 Findings from this study are likely to be of particular interest for practical applications in fisheries. Moreover,
235 the similarity of scaled body length distributions contribute to the advancement of life-history theory and
236 fitness optimization models^{4,6} which predict a narrow range of optimal body size distributions. Indeed, our
237 data suggest that in natural populations, over broad temporal and spatial scales, individual growth and life-
238 histories are optimized to maximize fitness.

239 Our study calls for concerted efforts to bring together diverse fish body size datasets to test predictions across
240 an even wider range of environmental conditions, as well as spatial and temporal scales. Further work is also
241 needed to test the sensitivity of the approach to the misspecification of statistical distribution (e.g., lognormal
242 or normal), sample sizes and conditions required to fit observations to the theoretical expectations with
243 sufficient accuracy. From an ecological perspective, it is important to understand whether, and how, the
244 observed variability in CV values (Fig. 2) and preferred distribution, especially smaller values in cryptobenthic
245 fishes, relates to environmental or phylogenetic factors, and whether they remain consistent across temporal
246 and spatial gradients within a species.

247 For data-poor and unassessed fishery species, which account for approximately 80% of all fishery species
248 worldwide³², size-based stock depletion assessments offer a key opportunity to improve our understanding of
249 the health of fish populations and associated requirements for sustainable fisheries management^{16,33,34}. This
250 opportunity is greatly upscaled by the now widespread availability of increasingly automated collections of fish
251 body size data. Findings from our study can support the use of these data by helping to quantitatively estimate
252 baseline (unfished) size frequency distributions without the need to parameterize highly uncertain rates of
253 growth and natural mortality^{17,35-37}. Observed size frequency distributions can then be contrasted to these
254 empirically-grounded expectations of unfished size frequency distributions to estimate population depletion.
255 Helping to better understand the status and management needs of unassessed fishery stocks addresses a
256 problem of global ecological and socio-economic significance, given that unassessed fish populations
257 worldwide are more likely to be in poor condition^{18,32,38-40}.

258

259 Methods

260 Body size data sources

261 We analyzed two datasets. The first dataset was obtained from underwater visual surveys around the
262 Australian continent (over 12 million individuals, 3,089 fish populations of 710 species) by divers in the Reef
263 Life Survey program (RLS)^{41,42} and the Australian Temperate Reef Collaboration (ATRC)⁴³. Visual census surveys
264 involved a standardized protocol of a diver searching 5m either side of a 50m transect line, recording
265 individual fish lengths to the nearest size bin (2.5, 5, 7.5, 10, 15, 20, 25, 30, ..., 400cm) and recording taxonomic
266 ID. Full details of the standardized methods are available online⁴⁴.

267 The second dataset was obtained from local-scale community collections of cryptobenthic fishes from
268 locations around the world (over 8000 individuals, 139 populations of 132 species)^{45,24,46}. Extractive sampling
269 of cryptobenthic fishes (CRF data) was performed in the field using enclosed clove-oil stations at six locations:
270 Mo'orea (French Polynesia), Fujairah (Gulf of Oman), Abu Dhabi (Arabian/Persian Gulf), Lizard Island
271 (Australia), Bocas del Toro (Panamá), and the Mesoamerican Barrier Reef in Belize. Detailed descriptions of the
272 collections across these locations are found in Brandl et al.^{45,24,46}. Reef outcrops were selected, measured, and
273 covered with a bell-shaped fine mesh and tarpaulin, before being sprayed with a clove-oil:ethanol solution
274 (1:5). Fish were collected with tweezers and placed in ziplock bags. In the laboratory, all fishes were measured
275 (nearest 0.1mm, and binned to 1mm bins for statistical distribution fitting – see *Statistical analysis*), weighed
276 (nearest 0.001g), photographed, and identified. See Brandl et al.²⁴ for full methods.

277 The majority (88%) of the data come from fish species that are unlikely to be targeted by either commercial or
278 recreational fishing, providing opportunities to investigate complete body sizes in close to natural unfished
279 populations. A population was defined as the collection of all individuals of a species within a location. For the
280 visual census datasets, to avoid biases associated with clumped survey-locations, we determined a 'location' to
281 be all surveys within a 1°x1° latitude-longitude grid cell (n = 3,089 populations). For the cryptobenthic fish
282 data, a location was defined as each sampled reef outcrop (n = 139 populations). When analyzing the influence
283 of spatial scale, for visual census data we also included a meta-population spatial scale, defined as all samples
284 within an ecoregion based on the Marine Ecoregions of the World²⁰. For both data sets we also included a
285 species level scale, where all data from a single species were pooled.

286 Data filtering

287 Before analyses data were filtered for errors by exploring unusual body sizes and out of area observations. For
288 visual census data, we further excluded populations where body size distributions spanned fewer than four
289 body size bins (e.g., spanning 2.5cm, 5cm, and 7.5cm size bins only) or where more than half of individuals
290 were in the smallest observable body size bin (i.e., 2.5cm bin). For the CRF data, where fish were measured
291 individually, we set a minimum number of 10 individuals per population to fit a distribution, for the visual
292 census data, where fish are counted in size bins, the minimum was set to 100 individuals. We performed a
293 sensitivity analysis to show that these filtering parameters had no significant influence on the overall CV
294 estimates (Extended Data Fig. 9).

295 Of the 3,089 visual census populations, 215 populations were not included in analyses when calculating the
296 coefficient of variation: 59 populations were removed prior to distribution-fitting due to bimodal distributions,
297 and 152 populations with greater than 50% of individuals within a single body size class. The removal of
298 bimodal distributions did not significantly influence the results (Extended Data Fig. 10).

299 **Statistical analysis**

300 The goal of our statistical analysis was to evaluate the suitability of the positive-normal (PN, i.e., truncated
301 normal) and lognormal (LN) probability density functions in describing the length-binned visual data for each
302 fish population, and the more accurately measured cryptobenthic species. For each population we identified
303 which of these two distributions better described the observed fish lengths and we also assessed whether the
304 mean of the better distribution informed its coefficient of variation in a consistent manner across species or
305 populations.

306 Consider a fish population of interest and let n_i denote the number of individuals observed within length-bin i ,
307 which is bounded by lengths l_i and l_{i+1} (cm). When assessing fish populations using data collected via
308 cryptobenthic sampling length data were associated with 1mm size bins. Let $F_m(l|\mu, \sigma)$ denote the cumulative
309 probability density associated with length distribution $m = \text{PN or LN}$. Here we have parameterized both length
310 distributions according to a central tendency parameter μ and a variance parameter σ . The probability of
311 observing a randomly selected fish being in length-bin i according to length distribution m is:

$$312 \quad P_i^m = k(F_m(l_{i+1}|\mu, \sigma) - F_m(l_i|\mu, \sigma)),$$

313 where k is the normalization constant, $k = 1/(1 - F_m(l_1|\mu, \sigma))$. The fish observations are not independent as
314 they have been collected at multiple locations and times. This non-independence will result in variation in
315 counts across length-bins being greater than expected according to the multinomial distribution. A common
316 way to account for non-independence and accommodate overdispersion is to assume that the counts
317 distributed across bins are consistent with the Dirichlet-multinomial distribution. According to this assumption
318 the likelihood of observing all the $n = \sum_i n_i$ fish counts is:

$$319 \quad L(\mu, \sigma, \theta_0) = \frac{\Gamma(\theta_0)\Gamma(n+1)}{\Gamma(n+\theta_0)} \prod_{i=1}^I \frac{\Gamma(n_i+\theta_i)}{\Gamma(\theta_i)\Gamma(n_i+1)},$$

320 where θ_0 is a positive constant describing the degree of overdispersion, and $\theta_i = \theta_0 P_i^m$.

321 For each population and both length distributions, the three parameters $\{\mu, \sigma, \theta_0\}$ were estimated using
322 Bayesian methods. We considered uninformative priors for all parameters and coded the likelihood using the
323 Stan programming language (implemented via the package 'rstan'). Convergence and estimation of the
324 posterior parameter distributions was performed using three chains of length 2,000 iterations (including a
325 1,000-iteration warmup). As both size-distribution models were described by the same number of parameters
326 (i.e. $\{\mu, \sigma, \theta_0\}$), we identified the better fitting size-distribution according to the highest median of the
327 marginal posterior log-likelihood. Of the 3,068 fitted populations, 9 did not converge for the lognormal
328 distribution but did for the normal, in which case the normal distribution was determined as the preferred
329 distribution, for all other populations convergence was achieved for both distributions. The posterior median
330 parameters: μ and σ , from the better fitting model, were then used to calculate the mean and the coefficient
331 of variation of fish lengths for the whole fish population.

332 All statistical analyses were performed using the statistical programming language R⁴⁷ in combination with the
333 Bayesian statistical modelling language Stan⁴⁸.

334 **Reconstructing the body size distribution from a single parameter**

335 Assuming a coefficient of variation of 0.34, and the mean body length of the population (\bar{L}), we can calculate
336 the two parameters of each of the lognormal and normal distribution (truncated at the smallest body size
337 observable; 1.25cm for visual census data). For the normal distribution, the mean of the distribution is equal to

338 the observed mean of the population, (\bar{L}), the standard deviation σ of the distribution is calculated equal to
339 $0.34\bar{L}$. For the lognormal distribution, if parameterized as $LN(\mu, \sigma^2)$, we can calculate σ as $\sqrt{\log(0.34^2 + 1)}$,
340 and μ as $\log(\bar{L} - \frac{\sigma^2}{2})$.

341 To reconstruct the natural population body length distribution from just asymptotic length (L_{inf}) for the
342 comparisons of performances between our simple model and a commonly used size-based population
343 assessment models LBSPR we used Prince et al. estimates of L_{inf} that were available for 68 mostly unfished
344 species in our dataset. The two size measures were correlated (Extended Data Fig. 10) ($R^2 = 74\%$) and mean
345 body sizes \bar{L} for the 68 species were estimated using empirically derived regression $\log(\bar{L}) = 0.37 + 0.78 \cdot$
346 $\log(L_{inf})$.

347 **Reconstructing body size distributions using LBSPR model**

348 To compare how our simple method of reconstructing body size distributions performed compared to
349 traditional fisheries population dynamics predictions, we used the commonly applied size based population
350 assessment method LBSPR (length-based spawning potential ratio)¹⁵, as implemented in the R package
351 LBSPR³³. The LBSPR method reconstructs expected size distributions using Beverton and Holt fisheries
352 population dynamics predictions¹⁴, assuming that fish growth follows the Von Bertalanffy growth model,
353 mortality at ages recruited to the fishery is constant, recruitment is continuous and the coefficient of variation
354 around length at age is 10%^{15,16}. The function 'LBSPRsim' from the LBSPR package was used to reconstruct
355 unfished length distribution using mortality and growth ratio (M/k) and asymptotic length (L_{inf}).

356 Species-level M, k, and L_{inf} were obtained from Prince et al.¹⁷. If multiple values of M and k were given for a
357 single species, the M and k combination with the closest M/k ratio to the median of the species was selected.
358 Only species that appeared in both the visual census dataset, had published M/k ratio and L_{inf} values from
359 Prince et al.¹⁷ and were deemed to be not intensively fished were selected (n = 68 species, including species
360 with some level of fishing in part of their geographic distribution). These 68 species were used to compare how
361 the model presented here (normal truncated size distribution with the CV around mean size of 0.34) and
362 LBSPR predict observed length frequencies using the same L_{inf} parameter (Fig. 4).

363 **Observed versus expected dissimilarity**

364 To compare between empirically observed and predicted body length distributions (e.g., normal versus LBSPR
365 expected in Fig.3, or normal versus lognormal in Fig. 4), we used the Kolmogorov-Smirnov (K-S) test. The K-S
366 test is a nonparametric test of equality between two distributions, in our case an observed and predicted body
367 length distribution. Here we use the K-S statistic (using the 'ks.test' function within the 'stats' package of R) as
368 a relative measure of dissimilarity between two samples (observed, and predicted, proportion in body length
369 bin).

370 **Code availability statement**

371 Data and code (R and stan) to recreate the figures in this study are available at
372 github.com/FreddieJH/size_dist_fitting (and will be archived on Zenodo before publication).

373 **Acknowledgements**

374 We thank the many Reef Life Survey divers and members of the Australian Temperate Reef Collaboration who
375 collected the visual census data used here. These data used in the analyses are managed through, and were

376 sourced from, Australia’s Integrated Marine Observing System (IMOS) – IMOS is enabled by the National
377 Collaborative Research Infrastructure Strategy (NCRIS). We also thank the many divers that assisted with
378 cryptobenthic fish collections. We also thank Rainer Froese, Ken Haste Andersen and Gustav Delius for
379 comments on the manuscript drafts, Michael Spence for efforts in improving computation speeds in Bayesian
380 modelling and Wanwan Kurniawan for help with the LBSPR model. This study was supported by the Australian
381 Research Council (ARC) Discovery Project (DP220102446) to AA, SAR and NCK, ARC Future Fellowship
382 (FT190100599) to RD S-S, and Pew Fellowships in Marine Conservation to AA and RD S-S.

383

384 References

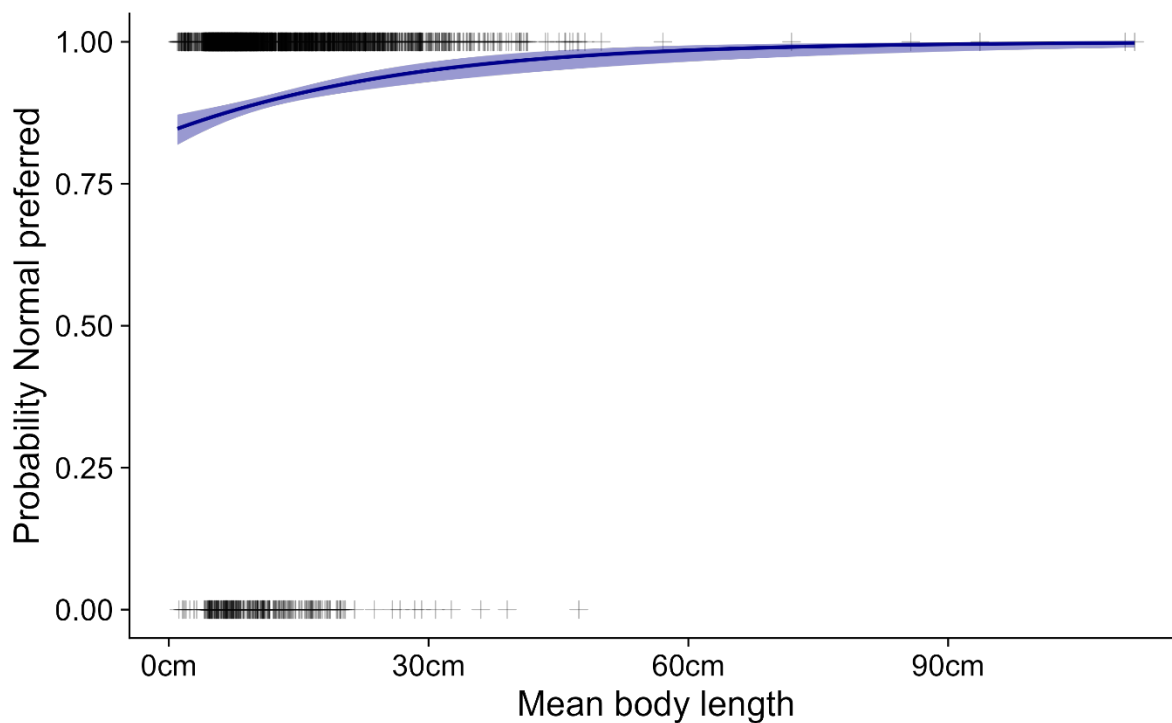
- 385 1. Andersen, K. H. *et al.* Characteristic Sizes of Life in the Oceans, from Bacteria to Whales. *Annu. Rev. Mar.*
386 *Sci.* **8**, 217–241 (2016).
- 387 2. Hordyk, A., Ono, K., Sainsbury, K., Loneragan, N. & Prince, J. Some explorations of the life history ratios to
388 describe length composition, spawning-per-recruit, and the spawning potential ratio. *ICES Journal of*
389 *Marine Science* **72**, 204–216 (2015).
- 390 3. Charnov, E. L., Turner, T. F. & Winemiller, K. O. Reproductive constraints and the evolution of life histories
391 with indeterminate growth. *Proc. Natl. Acad. Sci. U.S.A.* **98**, 9460–9464 (2001).
- 392 4. Jensen, A. L. Beverton and Holt life history invariants result from optimal trade-off of reproduction and
393 survival. (1996).
- 394 5. Beverton, R. & Holt, S. *A Review of the Lifespans and Mortality Rates of Fish in Nature, and Their Relation*
395 *to Growth and Other Physiological Characteristics*. vol. 5 (Wiley Online Library, 1959).
- 396 6. Charnov, E. L. *Life History Invariants: Some Explorations of Symmetry in Evolutionary Ecology*. (Oxford
397 University Press, 1993).
- 398 7. Jørgensen, C. & Holt, R. E. Natural mortality: Its ecology, how it shapes fish life histories, and why it may
399 be increased by fishing. *Journal of Sea Research* **75**, 8–18 (2013).
- 400 8. Dureuil, M. & Froese, R. A natural constant predicts survival to maximum age. *Commun Biol* **4**, 641 (2021).
- 401 9. Gislason, H., Daan, N., Rice, J. C. & Pope, J. G. Size, growth, temperature and the natural mortality of
402 marine fish: Natural mortality and size. *Fish and Fisheries* **11**, 149–158 (2010).
- 403 10. Healy, K., Ezard, T. H. G., Jones, O. R., Salguero-Gómez, R. & Buckley, Y. M. Animal life history is shaped by
404 the pace of life and the distribution of age-specific mortality and reproduction. *Nat Ecol Evol* **3**, 1217–1224
405 (2019).
- 406 11. Pauly, D. On the interrelationships between natural mortality, growth parameters, and mean
407 environmental temperature in 175 fish stocks. *ICES Journal of Marine Science* **39**, 175–192 (1980).
- 408 12. Prince, J., Hordyk, A., Valencia, S. R., Loneragan, N. & Sainsbury, K. Revisiting the concept of Beverton—
409 Holt life-history invariants with the aim of informing data-poor fisheries assessment. *ICES Journal of*
410 *Marine Science* **72**, 194–203 (2015).
- 411 13. Giometto, A., Altermatt, F., Carrara, F., Maritan, A. & Rinaldo, A. Scaling body size fluctuations. *Proc. Natl.*
412 *Acad. Sci. U.S.A.* **110**, 4646–4650 (2013).
- 413 14. Beverton, R. & Holt, S. *On the Dynamics of Exploited Fish Populations*. (Her Majesty’s Stationary Office,
414 1957).

- 415 15. Hordyk, A., Ono, K., Valencia, S., Loneragan, N. & Prince, J. A novel length-based empirical estimation
416 method of spawning potential ratio (SPR), and tests of its performance, for small-scale, data-poor
417 fisheries. *ICES Journal of Marine Science* **72**, 217–231 (2015).
- 418 16. Froese, R. *et al.* A new approach for estimating stock status from length frequency data. *ICES Journal of*
419 *Marine Science* **75**, 2004–2015 (2018).
- 420 17. Prince, J. D., Wilcox, C. & Hall, N. How to estimate life history ratios to simplify data-poor fisheries
421 assessment. *ICES Journal of Marine Science* **80**, 2619–2629 (2023).
- 422 18. FAO. *The State of World Fisheries and Aquaculture 2022*.
423 <http://www.fao.org/documents/card/en/c/cc0461en> (2022) doi:10.4060/cc0461en.
- 424 19. Brandl, S. J., Goatley, C. H. R., Bellwood, D. R. & Tornabene, L. The hidden half: ecology and evolution of
425 cryptobenthic fishes on coral reefs. *Biol Rev* **93**, 1846–1873 (2018).
- 426 20. Spalding, M. D. *et al.* Marine Ecoregions of the World: A Bioregionalization of Coastal and Shelf Areas.
427 *BioScience* **57**, 573–583 (2007).
- 428 21. Huston, M. A. & DeAngelis, D. L. Size Bimodality in Monospecific Populations: A Critical Review of Potential
429 Mechanisms. *The American Naturalist* **129**, 678–707 (1987).
- 430 22. Macdonald, P. D. M. & Pitcher, T. J. Age-Groups from Size-Frequency Data: A Versatile and Efficient
431 Method of Analyzing Distribution Mixtures. *J. Fish. Res. Bd. Can.* **36**, 987–1001 (1979).
- 432 23. Depczynski, M. & Bellwood, D. R. Extremes, plasticity, and invariance in vertebrate life history traits:
433 insights from coral reef fishes. *Ecology* **87**, 3119–3127 (2006).
- 434 24. Brandl, S. J. *et al.* Demographic dynamics of the smallest marine vertebrates fuel coral reef ecosystem
435 functioning. *Science* **364**, 1189–1192 (2019).
- 436 25. Thorson, J. T., Munch, S. B., Cope, J. M. & Gao, J. Predicting life history parameters for all fishes worldwide.
437 *Ecological Applications* **27**, 2262–2276 (2017).
- 438 26. Froese, R. & Binohlan, C. Empirical relationships to estimate asymptotic length, length at first maturity and
439 length at maximum yield per recruit in fishes, with a simple method to evaluate length frequency data.
440 *Journal of Fish Biology* **56**, 758–773 (2000).
- 441 27. Beverton, R. J. H. Patterns of reproductive strategy parameters in some marine teleost fishes. *Journal of*
442 *Fish Biology* **41**, 137–160 (1992).
- 443 28. Mangel, M. Invariant ratios vs. dimensionless ratios. *Science* **310**, 1426–1427 (2005).
- 444 29. Nee, S., Colegrave, N., West, S. A. & Grafen, A. The Illusion of Invariant Quantities in Life Histories. *Science*
445 **309**, 1236–1239 (2005).
- 446 30. Coulson, T., Gaillard, J. & Festa-Bianchet, M. Decomposing the variation in population growth into
447 contributions from multiple demographic rates. *Journal of Animal Ecology* **74**, 789–801 (2005).
- 448 31. Ackerman, J. & Bellwood, D. Reef fish assemblages: a re-evaluation using enclosed rotenone stations. *Mar.*
449 *Ecol. Prog. Ser.* **206**, 227–237 (2000).
- 450 32. Costello, C. *et al.* Status and Solutions for the World’s Unassessed Fisheries. *Science* **338**, 517–520 (2012).
- 451 33. Hordyk, A. Package LBSPR. (2019).
- 452 34. Rudd, M. B. & Thorson, J. T. Accounting for variable recruitment and fishing mortality in length-based
453 stock assessments for data-limited fisheries. *Can. J. Fish. Aquat. Sci.* **75**, 1019–1035 (2018).
- 454 35. Barnett, L. A. K., Branch, T. A., Ranasinghe, R. A. & Essington, T. E. Old-Growth Fishes Become Scarce under
455 Fishing. *Current Biology* **27**, 2843-2848.e2 (2017).

- 456 36. Froese, R. *et al.* On the pile-up effect and priors for Linf and M/K: response to a comment by Hordyk et al.
457 on “A new approach for estimating stock status from length frequency data”. *ICES Journal of Marine*
458 *Science* **76**, 461–465 (2019).
- 459 37. Hordyk, A. R., Prince, J. D., Carruthers, T. R. & Walters, C. J. Comment on “A new approach for estimating
460 stock status from length frequency data” by Froese et al. (2018). *ICES Journal of Marine Science* **76**, 457–
461 460 (2019).
- 462 38. Hilborn, R. *et al.* Effective fisheries management instrumental in improving fish stock status. *Proc. Natl.*
463 *Acad. Sci. U.S.A.* **117**, 2218–2224 (2020).
- 464 39. Hilborn, R. *et al.* State of the World’s Fisheries. *Annu. Rev. Environ. Resour.* **28**, 359–399 (2003).
- 465 40. Worm, B. *et al.* Rebuilding Global Fisheries. *Science* **325**, 578–585 (2009).
- 466 41. Edgar, G. J. *et al.* Establishing the ecological basis for conservation of shallow marine life using Reef Life
467 Survey. *Biological Conservation* **252**, 108855 (2020).
- 468 42. Edgar, G. J. & Stuart-Smith, R. D. Systematic global assessment of reef fish communities by the Reef Life
469 Survey program. *Sci Data* **1**, 140007 (2014).
- 470 43. Edgar, G. J. & Barrett, N. S. Effects of the declaration of marine reserves on Tasmanian reef fishes,
471 invertebrates and plants. *Journal of Experimental Marine Biology and Ecology* **242**, 107–144 (1999).
- 472 44. Reef Life Survey Foundation. Standardised Survey Procedures for Monitoring Rocky & Coral Reef
473 Ecological Communities. [https://reeflifesurvey.com/wp-content/uploads/2019/02/NEW-Methods-](https://reeflifesurvey.com/wp-content/uploads/2019/02/NEW-Methods-Manual_150815.pdf)
474 [Manual_150815.pdf](https://reeflifesurvey.com/wp-content/uploads/2019/02/NEW-Methods-Manual_150815.pdf) (2019).
- 475 45. Brandl, S. J., Casey, J. M., Knowlton, N. & Duffy, J. E. Marine dock pilings foster diverse, native
476 cryptobenthic fish assemblages across bioregions. *Ecology and Evolution* **7**, 7069–7079 (2017).
- 477 46. Brandl, S. J. *et al.* Extreme environmental conditions reduce coral reef fish biodiversity and productivity.
478 *Nat Commun* **11**, 3832 (2020).
- 479 47. R Core Team. *R: A Language and Environment for Statistical Computing*. (R Foundation for Statistical
480 Computing, Vienna, Austria, 2022).
- 481 48. Stan Development Team. Stan Modeling Language Users Guide and Reference Manual, v2.21.0. (2023).
- 482

483

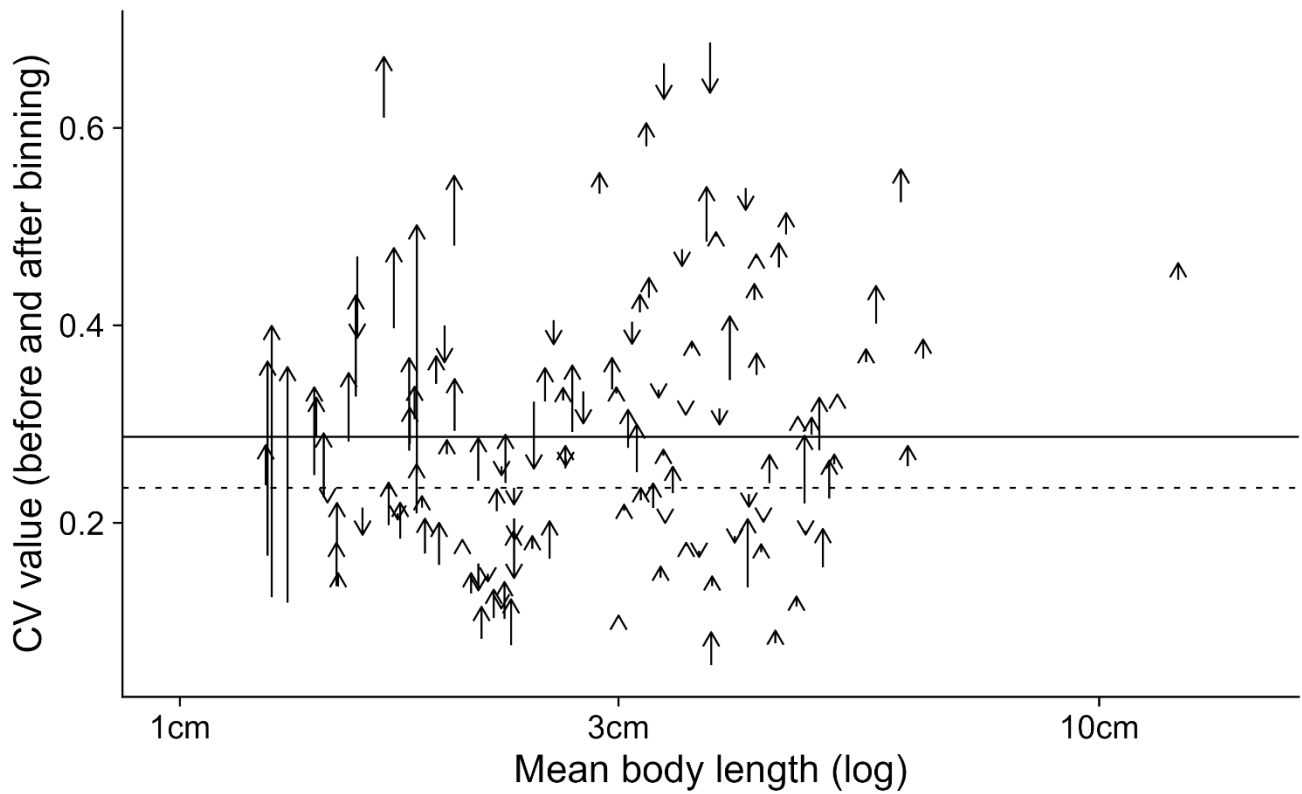
484 **Extended Data**



485

486 **Extended Data Figure 1.** Populations with larger mean body lengths are usually better described by a
487 truncated normal than a lognormal distribution. The blue line shows the logistic regression fit to the data. The
488 populations include both visual census and cryptobenthic data.

489

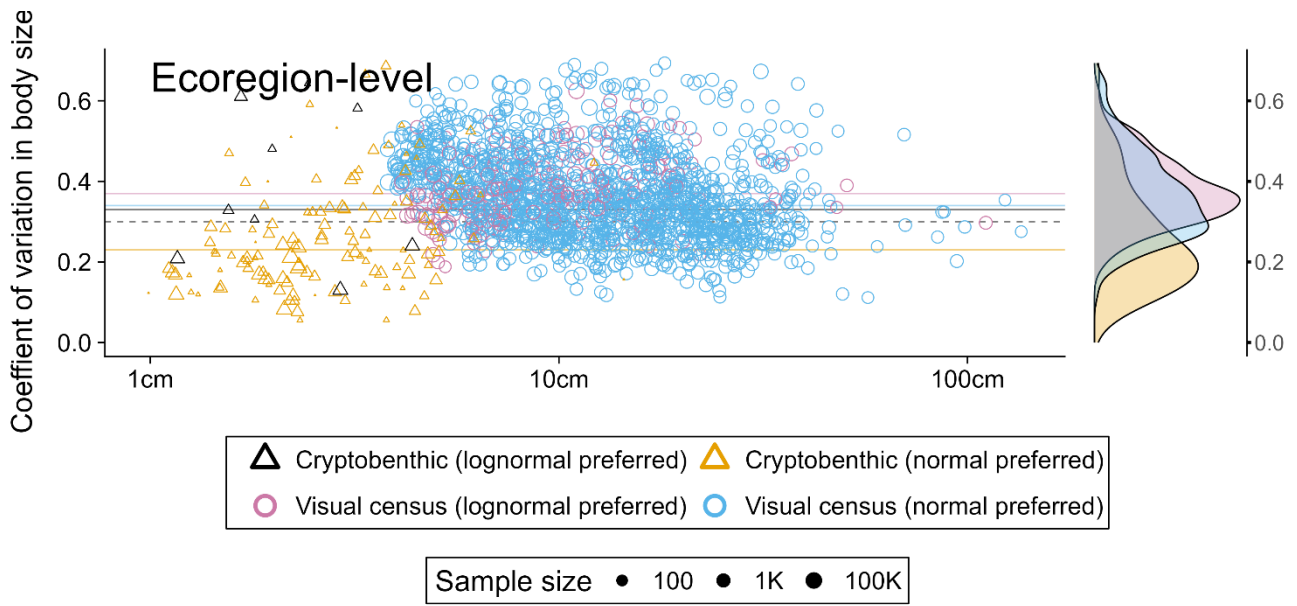


490

491 **Extended Data Figure 2.** Binning the cryptobenthic data (median CV = 0.23, dotted horizontal line) into visual
 492 census bins results in a greater median CV value (median CV = 0.28, solid horizontal line). Arrows represent the
 493 change from the CV value (either normal or lognormal) of the continuous data to the CV value of the binned
 494 data. Note: To be binned into the same visual census bins (2.5cm, 5cm, 7.5cm etc.), cryptobenthic body
 495 lengths were multiplied by a constant (constant = 3) before binning.

496

497



498

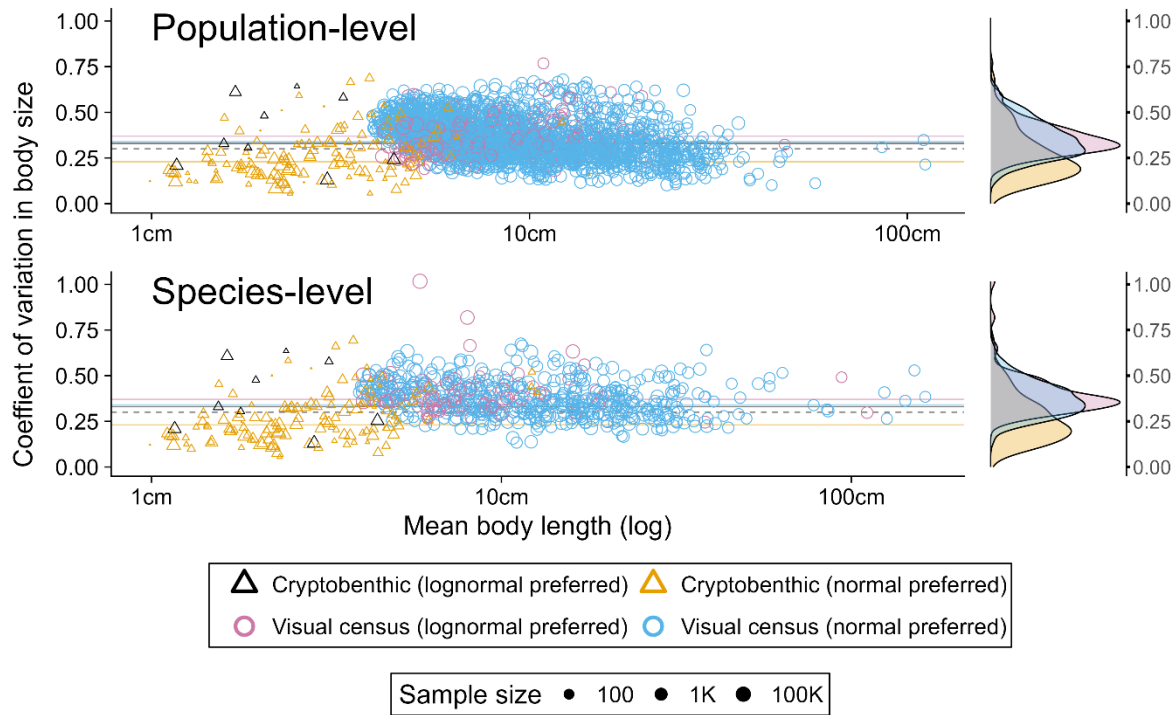
499 **Extended Data Figure 3.** Relationship between population mean body length and CV at the ecoregion-level in
 500 the visual census data and location level in the cryptobenthic data. Fisheries-targeted species and distributions
 501 deemed to be bimodal have been excluded. The median CV value is 0.35, 80% of CV values fall in the range of
 502 0.23 to 0.51 and 95% of the CV values fall in the range of 0.19 and 0.56.

503

504

505

506



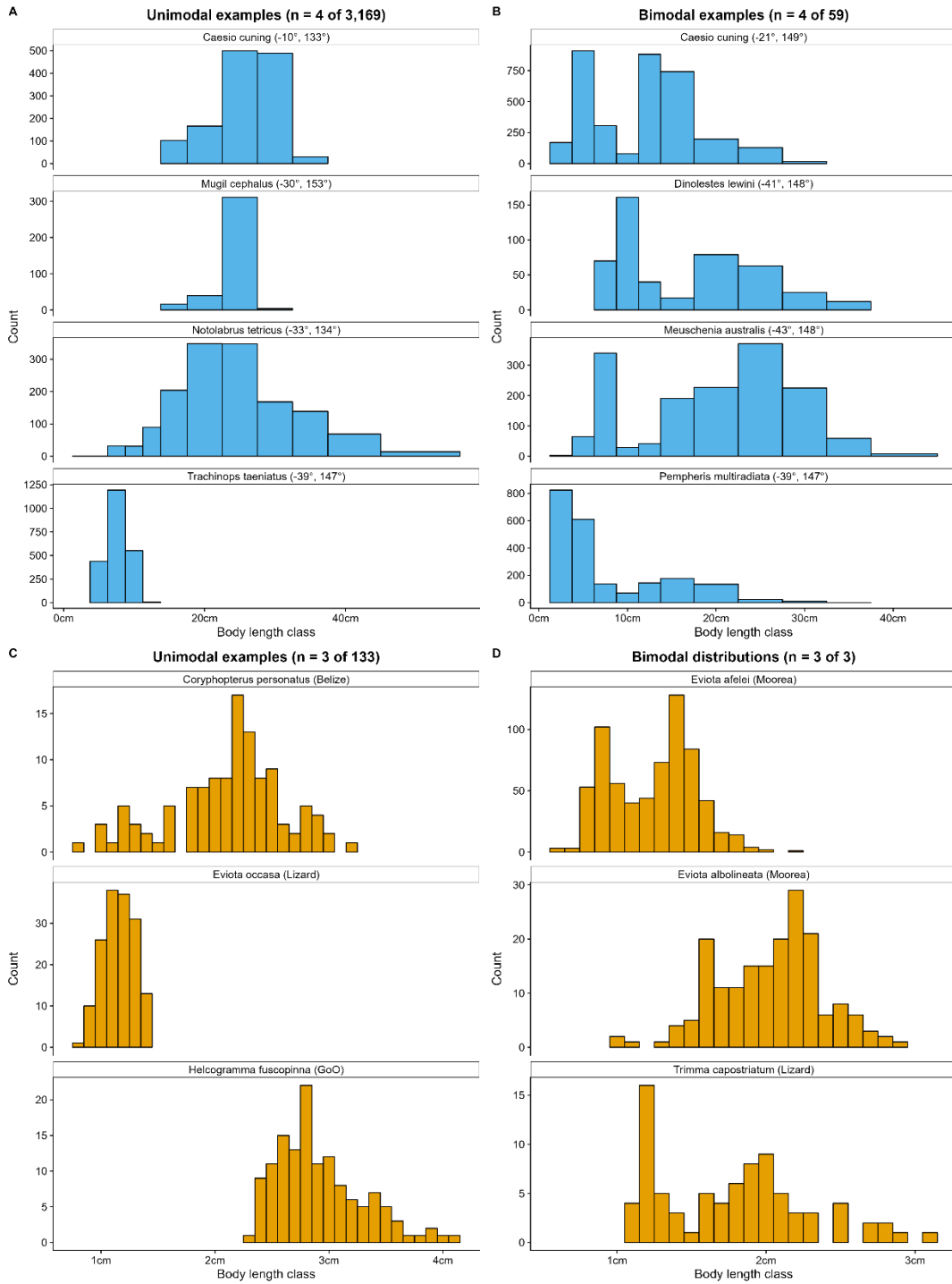
507

508 **Extended Data Figure 4.** Reconstruction of Fig. 2 of the main text but excluding species and genera that are
 509 potentially targeted by fishing. Excluding these species has almost no influence on the estimate of CV. At the
 510 population level the median CV value is 0.34, 80% of CV values fall in the range of 0.22 to 0.51 and 95% of the
 511 CV values fall in the range of 0.19 and 0.55. At the species-level the median CV value is 0.35, 80% of CV values
 512 fall in the range of 0.22 to 0.50 and 95% of the CV values fall in the range of 0.17 and 0.56.

513

514

515

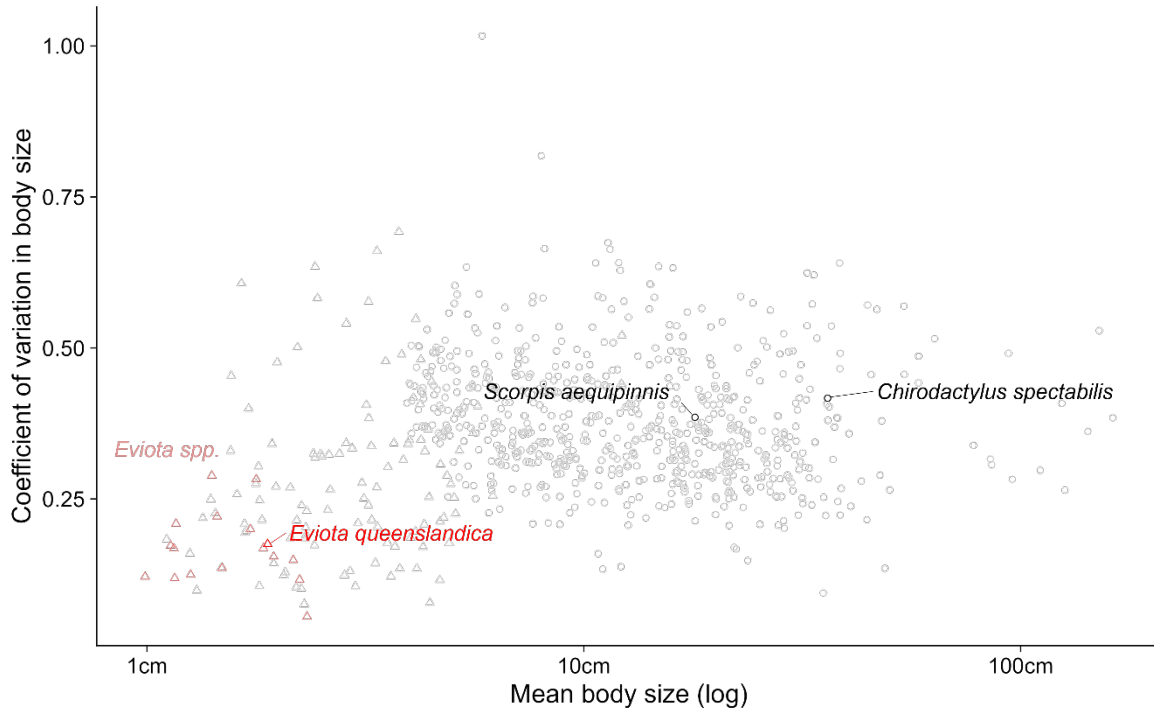


516

517 **Extended Data Figure 5.** Randomly selected examples of approximately unimodal (A, C) and bimodal (B, D)
 518 observed body length distributions in visual census sampling (blue, A, B) and cryptobenthic sampling (orange,
 519 C, D). Approximately bimodal shapes were found in 59 out of 3,089 (2%) of visual census, and 3 of 136 (2%)
 520 cryptobenthic population-level datasets. Bimodal distributions were removed from distribution-fitting
 521 analyses.

522

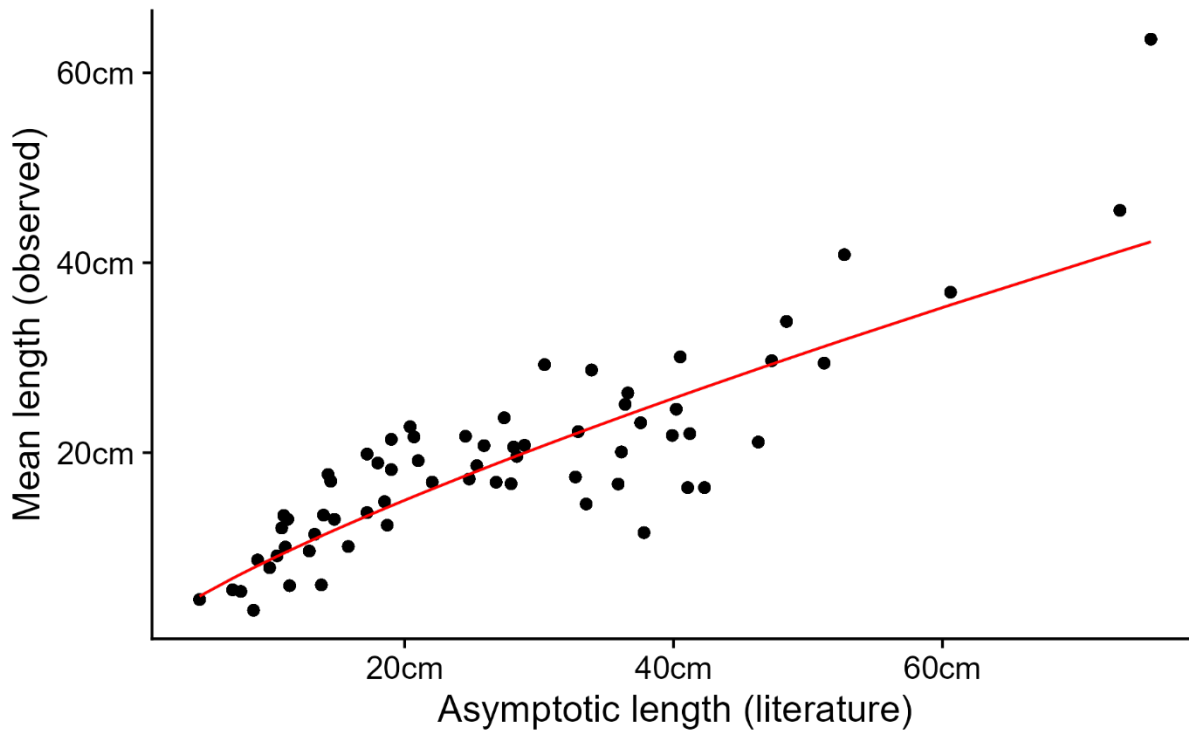
523



524

525 **Extended Data Figure 6.** Relationship between mean body length and coefficient of variation (CV), highlighting
526 three species with known extreme life-histories. The two species in black text are known to be long-lived, slow
527 growing species (*Scorpis aequipinnis* and *Chirodactylus spectabilis*), yet their CV values fall in the center of the
528 of the distribution of CV values. On the other hand, *Eviota spp.* and in particular, *E. queenslandica*, are known
529 to be fast-growing and short-lived. *Eviota spp.* are on the lower end of the range of CV estimates.

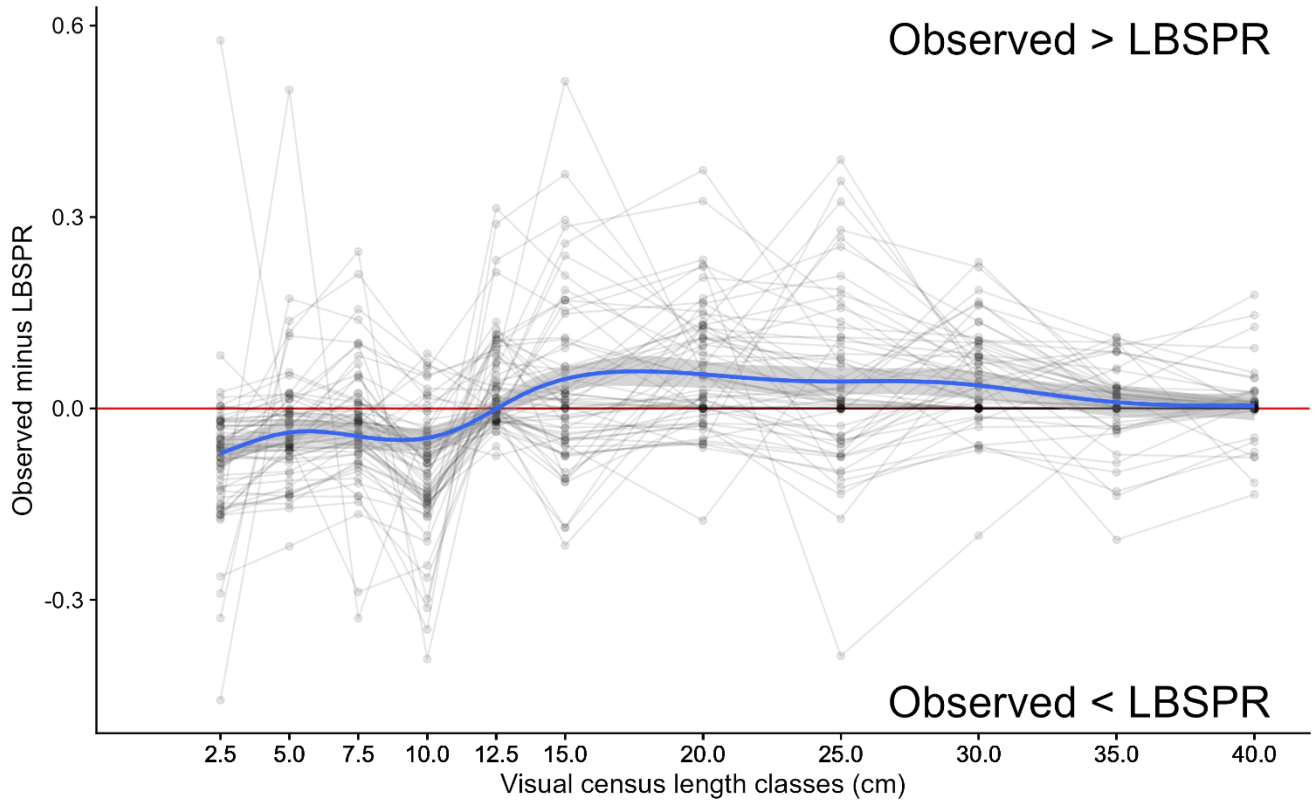
530



531

532 **Extended Data Figure 7.** A fitted linear model to predict mean population body length (from empirical body
533 length distributions) from asymptotic body length (available from Prince et al.¹⁷). This fitted model was used to
534 reconstruct the body length distribution when only asymptotic body length is known, which is often the case for
535 many species or populations. Fitted model (red line): $\log(\text{mean_length}) = 0.37 + 0.78 * \log(\text{asymptotic_length})$.

536



537

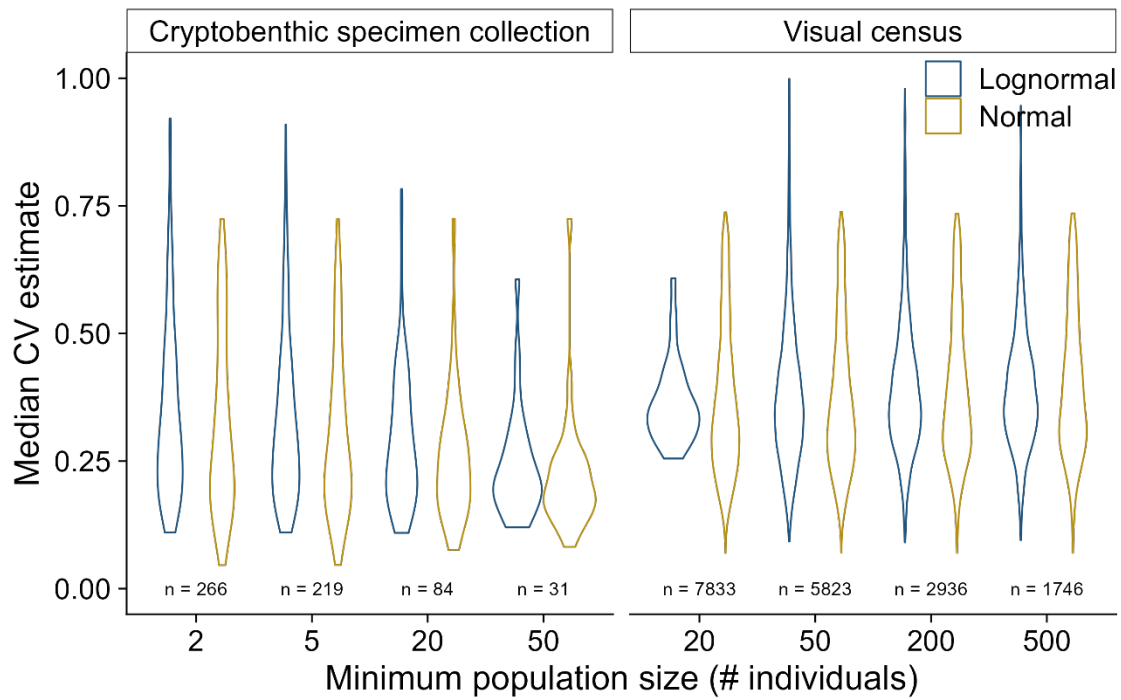
538 **Extended Data Figure 8.** Observed proportion within a length bin minus expected proportion as predicted by
 539 the theoretical model LBSPR. LBSPR is parameterized by asymptotic length, mortality (M) and growth rate (k).
 540 Points below the red horizontal line indicate there is a lower observed proportion of individuals in the size bin
 541 than predicted by LBSPR. The x-axis has been truncated to 40cm to emphasize this region where observational
 542 sampling bias is most likely to occur.

543

544

545

546



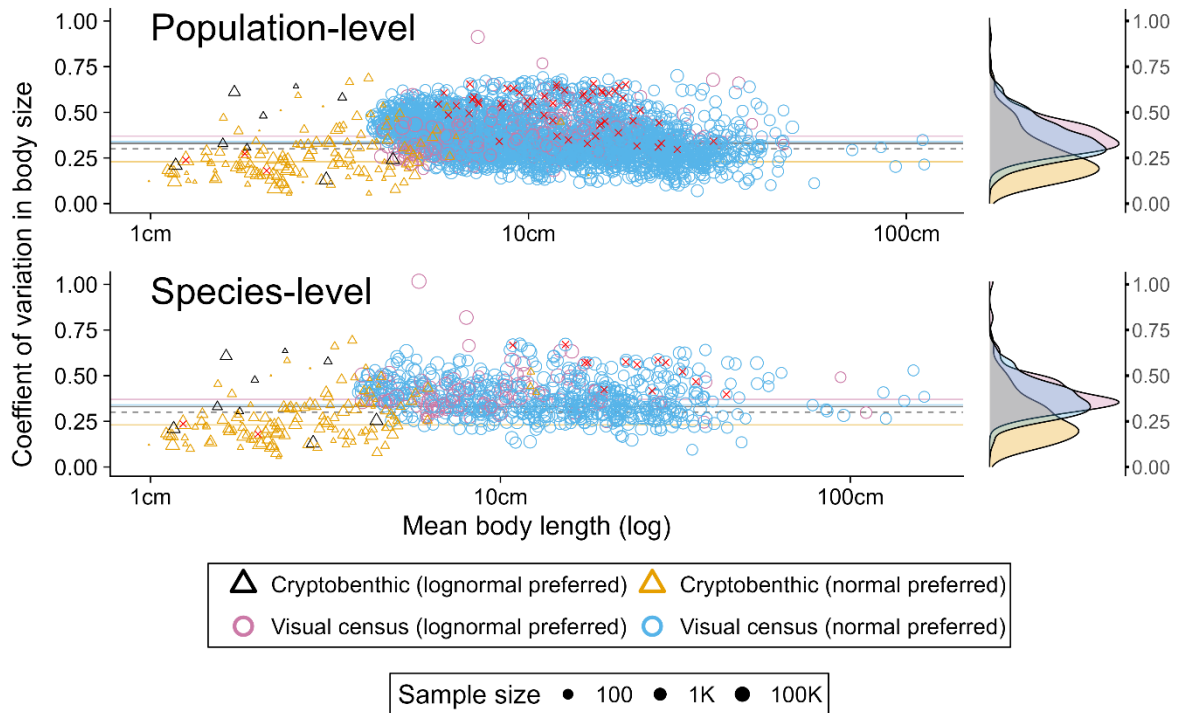
547

548 **Extended Data Figure 9.** Changing the minimum sample size (individuals within a population) required for
 549 distribution fitting has minimal influence of the median estimate of the coefficient of variation (CV). CV values
 550 greater than one have been excluded from this figure.

551

552

553



554

555 **Extended Data Figure 10.** Distributions deemed to be bimodal (red crosses, 2% of total populations) were
 556 excluded in Fig. 2 in the main text. Including these distributions has minor influence on the estimate of CV. At
 557 the population level the median CV value is 0.34, 80% of CV values fall in the range of 0.22 to 0.51 and 95% of
 558 the CV values fall in the range of 0.19 and 0.56. At the species-level the median CV value is 0.36, 80% of CV
 559 values fall in the range of 0.22 to 0.51 and 95% of the CV values fall in the range of 0.17 and 0.57.

560